

IDENTIFICATION AND QUANTIFICATION OF THE INTERACTION MECHANISMS BETWEEN THE CATIONIC SURFACTANT HDTMA-Br AND MONTMORILLONITE

PABLO M. NARANJO^{1,*}, EDGARDO L. SHAM^{1,2}, ENRIQUE RODRÍGUEZ CASTELLÓN³, ROSA M. TORRES SÁNCHEZ⁴, AND ELSA M. FARFÁN TORRES^{1,5}

¹ INIQUI (Instituto de Investigaciones para la Industria Química) – Av. Bolivia 5150 (A4408FVY) Salta, Argentina

² Fac. Ingeniería, Universidad Nacional de Salta, Av. Bolivia 5150 (A4408FVY) Salta, Argentina

³ Fac. Ciencias, Campus de Teatinos, Universidad de Málaga, Boulevard Louis Pasteur 29010, Málaga, España

⁴ CETMIC (Centro de Tecnología en Minerales y Cerámica) – Camino Centenario y 506 CC (49) (B1897ZCA) M. B. Gonnet, Argentina

⁵ Fac. Cs. Exactas, Universidad Nacional de Salta, Av. Bolivia 5150 (A4408FVY) Salta, Argentina

Abstract—Several detailed studies have been done on the characterization of organoclays and the type of structures developed when they interact with alkylammonium molecules. Few published contributions exist, however, on the distribution of surfactant within the organoclays and the mechanism by which they are intercalated. Also, although X-ray photoelectron spectroscopy (XPS) is a suitable technique for the study of the surface characteristics of organoclays, very few such XPS studies have been carried out. With the aim of contributing to a better understanding of the intercalation process, a series of organoclays was synthesized using a montmorillonite and the cationic surfactant hexadecyltrimethylammonium bromide (HDTMA⁺Br⁻), with an increasing surfactant load of between 0.2 and 4.0 times the cation exchange capacity of the starting clay. By means of XPS, zeta potential, and thermal analysis techniques, distinguishing the strongly interacting fraction from the weakly interaction fraction of the adsorbed surfactant molecules was possible. Adsorption isotherms of each of these processes were constructed and then adjusted using the Langmuir and Dubinin-Radusquevich adsorption models. Three types of interaction between the surfactant and the clay were identified and described qualitatively and quantitatively. Two of these interactions, strong and weak, involved the hexadecyltrimethylammonium cation (HDTMA⁺). The third was a weak interaction involving the ion pair HDTMA⁺Br⁻. The results of this study may be useful for the comprehensive design of organoclays with specific physicochemical properties according to the application for which they are destined.

Key Words—Alkylammonium molecules, Cationic surfactant HDTMA-Br, Montmorillonite.

INTRODUCTION

Smectites are layered aluminosilicates generally arranged in groups of different numbers of layers. The layers have an excess negative charge in their structure. Cations which compensate these charges are located in the interlayer space, are referred to as ‘interlaminal cations’, and can be exchanged, either for organic or inorganic cations.

Organically modified clays, also known as organoclays or nanoclays, can be used in a number of ways, *e.g.* in catalytic processes, as rheological control agents in paintings and lubricants; to reinforce the matrix of polymers and plastics; as adsorbents for effluent treatments, in oil spills, releasing active matrix, *etc.* (Azejjel *et al.*, 2009; Carrado, 2000; de Paiva *et al.*, 2008).

The use of thermal analysis techniques for the study of montmorillonitic clays is well established. Thermoanalytical studies of organo-modified clays

have demonstrated the applicability of differential thermal analysis-thermogravimetry (DTA-TG) and differential scanning calorimetry (DSC) for differentiating between adsorbed and free organic matter, and also between ionic and molecular adsorption (Xi *et al.*, 2005; He *et al.*, 2005, 2006; Yariv *et al.*, 2012).

X-ray photoelectron spectroscopy is a powerful technique for studying the surface characteristics of various materials, including clay minerals and related products. Unfortunately, to date, very few XPS studies of organoclays have been published, even though XPS provides valuable information about the distribution of surfactants within organoclays (He *et al.*, 2007).

Some of the studies published have described more than one type of interaction between the surfactants and the surface. When dealing with cationic surfactants, cationic exchange is reported as the most important mechanism of adsorption (Bilgiç, 2005). This type of adsorption is related to an average energy of adsorption of between 9 and 16 kJ/mol (Donat *et al.*, 2005). Another reported mechanism of adsorption is interaction through Van der Waals forces. This interaction is weaker than cation exchange adsorption, presenting average adsorption energies in the range 1–8 kJ/mol. Surfactant molecules can be adsorbed by the latter mechanism

* E-mail address of corresponding author:

pnanranjo@unsa.edu.ar

DOI: 10.1346/CCMN.2013.0610208

1 either as cations or as ion pairs with the respective
2 counterion (Tahani *et al.*, 1999).

3 To the authors' knowledge no work has been reported
4 that quantifies the fractions of surfactant adsorbed by the
5 different types of interaction.

6 The aim of the present study was to assess,
7 qualitatively and quantitatively, different mechanisms
8 of interaction between a HDTMA-Br type cationic
9 surfactant and the surface of a montmorillonite-type
10 clay mineral, and to propose the mechanisms involved in
11 these processes.

12 MATERIALS AND METHODS

13 *Materials*

14 Natural Castiglione clay, which consists mainly of
15 montmorillonite and has a cation exchange capacity
16 (CEC) of 83.7 mmol/100 g, together with hexadecyl-
17 trimethylammonium bromide (HDTMA-Br), provided
18 by Merck, were used as starting materials. All solutions
19 were prepared using deionized water (DI-H₂O)

20 *Preparation of organoclays*

21 Organoclays with surfactant loading (SL) of between
22 0.2 and 4.0 times the CEC were synthesized. The
23 synthesis was carried out in batch, putting 50 mL of a
24 suspension of ~5% w/v of the starting clay in contact with
25 different volumes of 5×10^{-3} M solution of HDTMA-Br,
26 in a final volume of 500 mL. This suspension was kept
27 under shaking for 2 h at room temperature. The solid
28 fraction (organoclay) was separated by centrifugation and
29 washed with DI-H₂O until the total elimination of Br⁻.
30 Organoclays were dried at 60°C, milled in an agate mortar
31 and stored in a desiccator for further characterization,
32 designating each of them as Bent followed by SL
33 (Bent-0.4, Bent-0.8, *etc.*).

34 *Characterization of the samples*

35 The intercalation process was analyzed by measuring
36 the concentration of the Br⁻ remaining in the solution
37 after the intercalation, which was achieved by precipita-
38 tion titration with a standard solution of 0.01 M AgNO₃
39 and 5% w/v K₂CrO₄ solution as indicator. At the same
40 time, the amount of Na⁺ exchanged in the solution was
41 quantified by atomic absorption spectrometry (AAS)
42 with flame ionization.

43 Thermogravimetric analyses were performed using a
44 Rigaku TAS 1100 instrument at temperatures ranging
45 from room temperature to 1200°C, at a heating rate of
46 20°C/min using 20 mg of sample, in a static air
47 atmosphere.

48 The starting clay mineral, solid surfactant, and
49 organoclays with SL of 0.4, 0.8, 2.0, and 4.0 were
50 analyzed by XPS, using an ESCA 5700 instrument from
51 'Physical Electronic' (University of Málaga, Málaga,
52 Spain), with MgK α and AlK α radiation ($h\nu = 1253.6$ and
53 1486.6 eV, respectively), using a hemispheric electron

1 analyser. Binding energies (BE) were determined with
2 an accuracy of ± 0.1 eV. Charge referencing was
3 measured against adventitious carbon (C1s =
4 284.8 eV). The residual pressure in the analysis chamber
5 was maintained below 10^{-7} Pa during all measurements.

6 Zeta potential (ζ) measurements of the starting clay
7 and the organoclay Bent 0.8 were performed in a Z-
8 Meter 3.0 instrument from NNN (National University of
9 Salta, Salta, Argentina), using suspensions of samples of
10 0.005% w/v in 0.01 M NaNO₃.

11 Adsorption isotherms were adjusted using the
12 Langmuir equation.

$$13 \quad q_e = q_{\max} * K_L * C_e / (1 + K_L * C_e) \quad (1)$$

14 where q_e is the amount of solute adsorbed per unit of
15 solid mass (mol/g) for an equilibrium concentration
16 C_e (mol/L); q_{\max} is the maximum amount adsorbed in
17 the surface (mol/g), and K_L is the Langmuir constant
18 (L/mol). From the Langmuir constant, a parameter, r ,
19 referred to as a "dimensionless equilibrium parameter"
20 can be calculated (Mahramanlioglu *et al.*, 2002). A value
21 of $r > 1$ indicates favorable adsorption, while $r < 1$
22 indicates an unfavorable adsorption. This parameter was
23 calculated as follows:

$$24 \quad r = 1 / (1 + K_L * C_0) \quad (2)$$

25 where C_0 is the value of the initial concentration of one
26 of the isotherm points.

27 These data were also adjusted using the Dubinin-
28 Radoskevich equation:

$$29 \quad q_e = q_{\max} \exp(-\beta \varepsilon^2) \quad (3)$$

30 where ε is the Polanyi potential:

$$31 \quad \varepsilon = RT \ln(1 - 1/C_e) \quad (4)$$

32 q_e , q_{\max} , and C_e have the same meanings as in the
33 previous equation and β (mol²/J²) is a constant related to
34 the average adsorption free energy (E , J/mol):

$$35 \quad E = - (2\beta)^{(-1/2)} \quad (5)$$

36 This last isotherm is more general than the Langmuir
37 isotherm because it assumes neither homogeneity of
38 surface adsorption sites nor constancy of adsorption
39 potential (Ackay *et al.*, 2006). The magnitude of
40 adsorption energy can give an indication of the type of
41 adsorption which occurred.

42 RESULTS AND DISCUSSION

43 Previous results showed that surfactant is adsorbed by
44 the Bent clay in at least two kinds of different sites
45 indicated by the different thermal stabilities of surfactant
46 molecules.

47 From characterization results and molecular model-
48 ing calculations, a mechanism of adsorption was
49 proposed. Surfactant molecules were initially adsorbed
50 in sites located in the interlayer space of the clay through
51

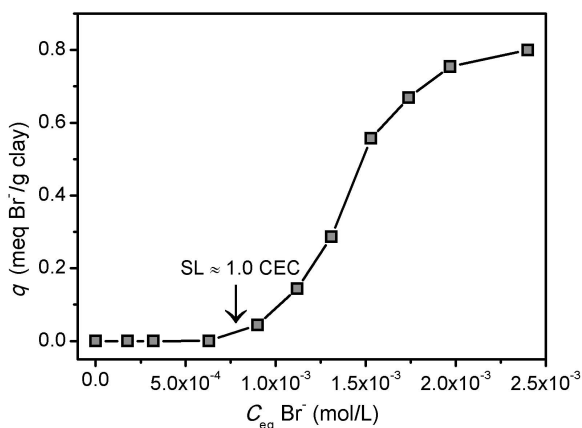


Figure 1. Sorption isotherms of bromide in montmorillonite.

cation exchange. In these kinds of sites, the adsorption was carried out until the interlayer space was saturated. Depending on the surfactant loading anchored in the intercalation process, different kinds of organization of the interlayer were obtained, varying from monolayer in Bent-0.4 to bilayer/pseudo-trilayer in Bent-3.0.

Further adsorption of surfactant occurred in the mesopores generated by tactoids ordered in a 'house-of-cards' type structure. This process left surfactant molecules relatively free, outside the interlayer space.

Quantification of Br^- and Na^+ in supernatant solution of adsorption isotherms

The Br^- anion is present during the adsorption process as a counterion of the cationic surfactant. Chemical analysis, performed after alkylammonium adsorption, showed that in the case of organoclays with SL up to ~ 1.0 CEC, all the initial Br^- stayed in the solution. For SL values > 1.0 CEC, a fraction of Br^- was adsorbed in the solid.

The sorption isotherm of Br^- (Figure 1) coincided with the S-type isotherm described by Giles *et al.* (1974), indicating that it is a system with low affinity of adsorbate for adsorbent. This is concurrent with the existing electrostatic repulsion between the structural negative charges of the layer and the bromide anion. When the SL is > 1.0 CEC (Figure 1), the negative charge is compensated by an excess of cationic surfactant, and the process of Br^- sorption begins. A similar phenomenon was observed by Su *et al.* (2012) for NO_3^- adsorption in reversed-charge smectites.

The amount of Na^+ released from the clay, as a result of cationic exchange with the surfactant, was also determined. Results show that the amount of Na^+ released increased with SL up to 1.0 CEC, and remained constant for higher SL values.

Thermogravimetric analysis

Up to $\sim 120^\circ\text{C}$, the starting clay experienced a mass loss corresponding to the elimination of physisorbed water, and then a second mass loss corresponding to the dehydroxylation of layers between 500 and 700°C (Figure 2a). Both thermal events are associated with several endothermic peaks detected in the DTA thermogram (Figure 2b). In organoclay thermograms, a mass loss related to the elimination of physisorbed water was observed between room temperature and $\sim 120^\circ\text{C}$ (Figure 2a). Another mass loss, associated with a series of exothermic events, was observed between 180 and 700°C , corresponding both to surfactant combustion phenomena and to the dehydroxylation of layers.

The total percentage of organic compound adsorbed by the clay as function of the SL was determined from thermograms. According to previous results, distinguishing the amount of surfactant adsorbed through each of the two mechanisms, based on the adsorption energies, is possible. The fraction with lower sorption energy

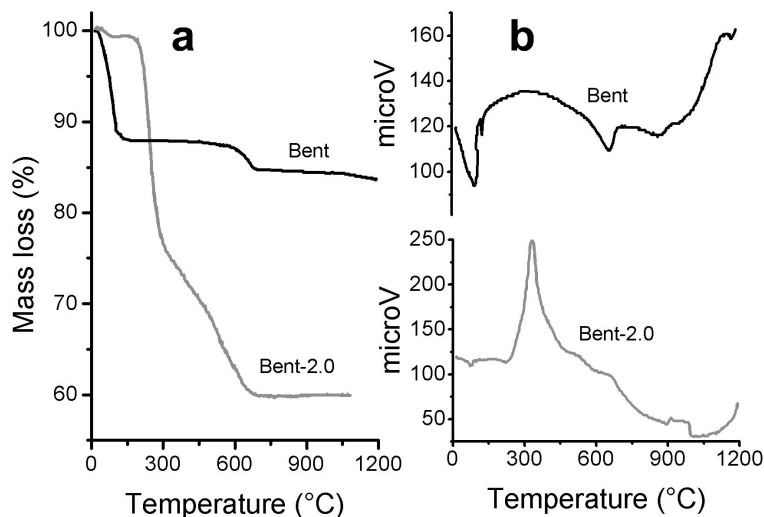


Figure 2. TG (a) and ATD (b) thermograms of Bent (black) and Bent-2.0 (gray).

(mechanism 1) is removed between 180 and 350°C, and the fraction with greater sorption energy (mechanism 2), between 350 and 800°C (Figure 3).

For mechanism 1, the adsorption isotherm slope decreased as the equilibrium concentration of the surfactant increased. It was a C-type isotherm in the Giles classification, indicating that the affinity between the solute and the solid was weak, consistent with the low temperatures at which this fraction of surfactant was eliminated (between 180 and 350°C). For mechanism 2, the isotherm slope increased vertically up to ~0.7 mmol surfactant/g clay and then remained almost constant. This was an H-type isotherm in the Giles classification, with high affinity between the solute and the adsorbent and with high adsorption energy, consistent with the higher temperature of elimination of this fraction of surfactant (between 350 and 800°C). The total adsorption isotherm is produced from the addition of these two isotherms.

Adjustment of adsorption isotherms

Data from adsorption isotherms of the surfactant adsorbed by each mechanism type and the total adsorbed were adjusted using the Langmuir and Dubinin-Raduskevich equations (Figure 3). The results obtained are summarized in Table 1.

Langmuir adsorption model. From the Langmuir adsorption model, values of q_{\max} for the total adsorbed amount ($q_{\max, \text{Total}}$) and for the amount adsorbed in weak sites through mechanism 1 ($q_{\max, 1}$) were calculated. For strong sites, a poor adjustment of the Langmuir equation was obtained ($R^2 = 0.4930$). This is related to the kind of adsorption process developed for the interactions with strong sites. Therefore, the value of q_{\max} for mechanism 2 ($q_{\max, 2}$) was obtained from the difference: $q_{\max, 2} = q_{\max, \text{Total}} - q_{\max, 1}$. A dimensionless equilibrium parameter was calculated using the concentration value of the first point of the adsorption isotherm (1.6×10^{-4} M). A value of $r < 1$ was found in each case, indicating that both adsorption mechanisms were favored.

Dubinin-Raduskevich adsorption model. From the Dubinin-Raduskevich adsorption model, the values of average adsorption energy for the total adsorption of

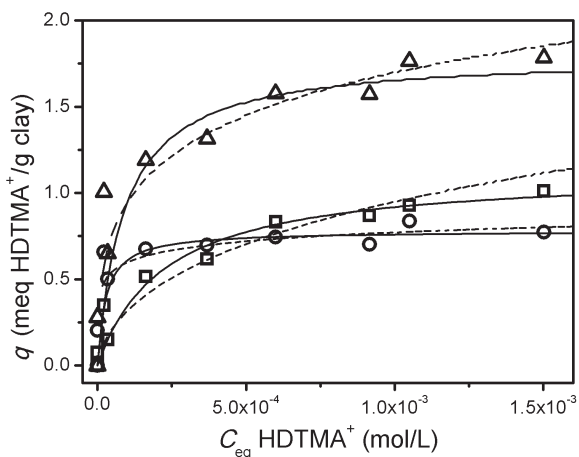


Figure 3. Adsorption isotherms of surfactant in clay by mechanism 1 (○), mechanism 2 (□) and total adsorption (△). Experimental data were adjusted by Langmuir (solid line) and Dubinin-Raduskevich (dash line) models.

surfactant ($E_{\text{Total}} = 12.8$ kJ/mol), the surfactant adsorbed through mechanism 1 (weak adsorption, $E_1 = 9.3$ kJ/mol), and the surfactant adsorbed through mechanism 2 (strong adsorption, $E_2 = 19.3$ kJ/mol) were obtained.

An average adsorption energy of between 1 and 8 kJ/mol indicated physisorption, and between 9 and 16 kJ/mol, chemical adsorption (Donat *et al.*, 2005). In the present study, the adsorption on strong sites was a process involving a slightly higher adsorption energy than is generally the case in processes of cationic exchange, so it may be a specific adsorption type, probably resulting in the formation of an inner sphere complex between the surfactant molecule and the clay mineral layer. Besides, the adsorption on weak sites practically coincided with the physisorption energy, meaning that mechanism 1 is the result of the adsorption, through Van der Waals forces (VdW), of surfactant molecules previously adsorbed in the clay by the strong mechanism.

XPS

Sodium and bromine. The results obtained showed the presence of Na in the starting clay, as characterized by the band at 1072.9 eV. In organoclays, the intensity of

Table 1. Langmuir and Dubinin-Raduskevich parameters for mechanism 1, mechanism 2, and the total adsorption.

Mechanism	Dubinin-Raduskevich isotherm			Langmuir isotherm				
	E_{ads} (kJ/mol)	R^2	N	q_m (mmol/g)	K_L (l/mol)	R^2	r	N
2 (strong)	19.3	0.8765	7	0.67*	–	–	–	–
1 (weak)	9.3	0.9642	7	1.13	4.39E+03	0.9970	0.59	7
Total	12.8	0.9744	7	1.80	1.10E+04	0.8695	0.36	7

* Value obtained by difference between $q_{\max, \text{Total}}$ and $q_{\max, 1}$.

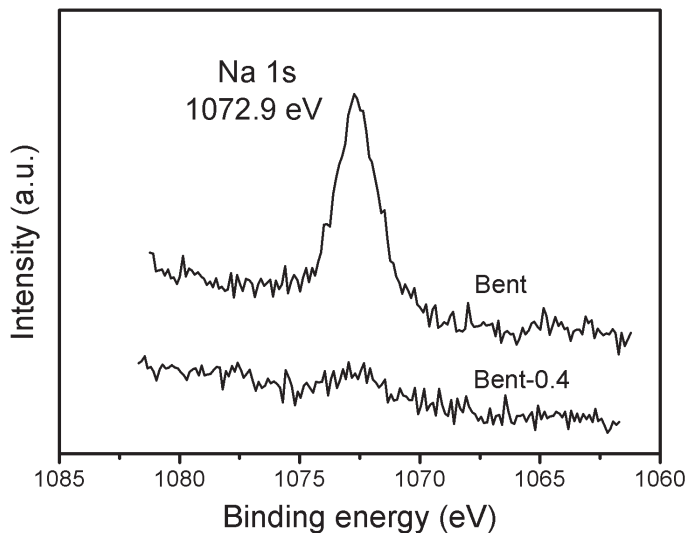


Figure 4. XPS spectra for the samples Bent and Bent-0.4 in the range 1060–1085 eV.

the band corresponding to Na decreased as SL increased. For a SL of 0.8 CEC, only traces of Na were detected, and Na was absent from organoclays with greater SL values as well as for pure surfactant (Figure 4).

The band corresponding to bromine in the XPS spectrum of HDTMA-Br was found at 67.0 eV. Its presence was detected in organoclays with SL values of 2.0 and 4.0 CEC, at 67.7 eV and 67.5 eV, respectively, but was absent from organoclays with lower SL values (Figure 5).

For a given element, binding energy (BE) increases when oxidation occurs, and decreases with reduction. The bromide anion adsorption starts when HDTMA⁺ adsorption exceeds the CEC. In this situation, Br⁻ anions were surrounded by an excess of cations, which

removed electron density. This decrease of electron density in the anion bromide is equivalent to ‘oxidation,’ coinciding with the observed increase in BE.

Nitrogen. Most nitrogen functions in which nitrogen is bound to carbon, like amine, amide, nitrile, urea, and nitrogen in aromatic rings, show N1s binding energies in the range 399–400 eV. Quaternary nitrogen shows greater binding energies in the range 401.5–402.5 eV, as expected from the localized positive charge (Briggs, 1998; Liu *et al.*, 2010).

HDTMA-Br presented a band corresponding to N1s at 402.1 eV, referred to as B1 in the present study. In organoclays, B1 shifted to values between 402.2 and

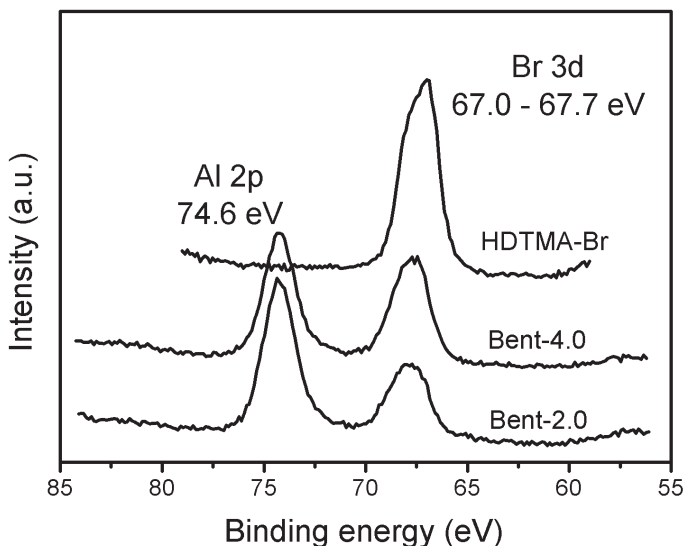


Figure 5. XPS spectra for the samples Bent-2.0, Bent-4.0, and for the pure surfactant in the range 55–85 eV.

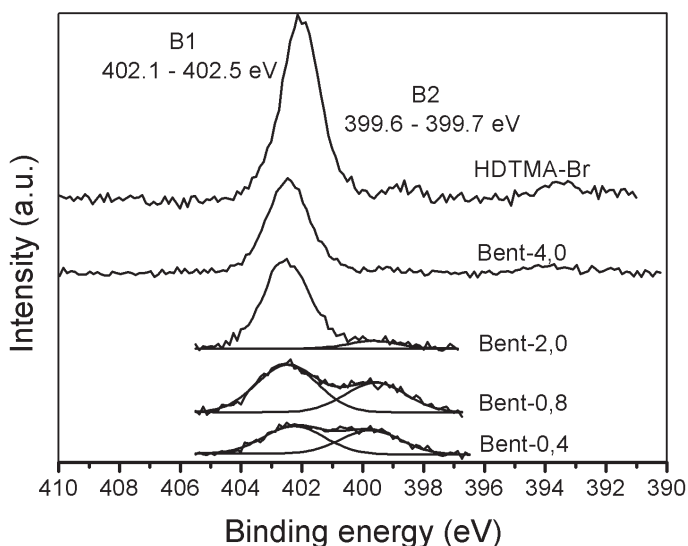


Figure 6. XPS spectra for the samples indicated in the range 390–410 eV.

402.5 eV. The XPS spectra of organoclays showed another band, referred to as ‘B2’ here, at values of between 399.6 and 399.7 eV (Figure 6).

The position of the B1 band coincides with the BE range of the quaternary nitrogen N1s band, so it was assigned to nitrogen atoms of the surfactant molecules adsorbed in the surface with low energy through Van der Waals forces, as was described for mechanism 1. On other hand, the position of the B2 band was assigned to nitrogen atoms adsorbed with high energy, and corresponds to surfactant molecules adsorbed through mechanism 2 (strong adsorption). The B2 band was not detected in the organoclay with the greatest SL value.

The decrease in binding energy of the B2 band indicated an increase of electron density in the nitrogen. This phenomenon occurs due to a charge transfer from the clay sheets to the surfactant molecule (Seki and Yurdakoç, 2005).

In order to facilitate the study of these results and to analyze them together with data provided by thermogravimetric analysis, the following ratios were defined:

$$R_{i, (B1/(B1+B2))} = A_{i, B1} / (A_{i, B1} + A_{i, B2})$$

$$R_{i, (IC/IC+VdW)} = q_{i, VdW} / (q_{i, IC} + q_{i, VdW})$$

where a_i is the area of the nitrogen XPS band (B1 or B2, as indicated) of the organoclay with SL = i and q_i is the amount of surfactant adsorbed per mass unit, as determined by TG, corresponding to adsorption by cationic exchange (CE) or by Van der Waals (VdW) interactions of the organoclay with SL = i .

Both ratios increased with SL (Figure 7). This indicates that the relative amount of molecules adsorbed through Van der Waals forces increased with SL. For small SL values, the TG results indicated that 20% of the molecules were adsorbed by Van der Waals interactions,

whereas XPS results indicated that this percentage is 50%. For large SL values, the percentage of molecules adsorbed by weak forces increased to 60%, according to TG, whereas, according to XPS, 100% of the molecules were observed to be adsorbed by Van der Waals interactions, *i.e.* molecules adsorbed through CE were not detected. The TG provided data about all of the sample, whereas XPS analyzes the surface only up to a determined depth (~4 nm in this case). So, the fact that molecules adsorbed through CE were not detected by XPS analyses in organoclays with SL = 4.0 CEC confirms that weak adsorption is produced at the external surface of the layers. The presence, in the interlayer space, of molecules fixed through strong adsorption could not be detected from XPS spectra

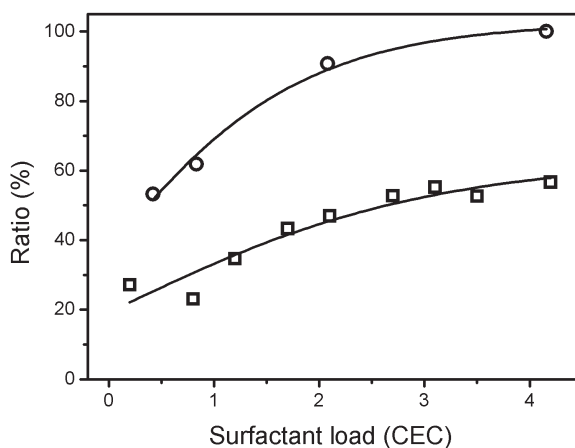


Figure 7. Percentage of surfactant adsorption by a weak mechanism with respect to total adsorption: data obtained from TG (\square) and XPS (\circ) are compared.

1 because of the limited depth of analysis in the conditions
2 in which these studies were carried out.

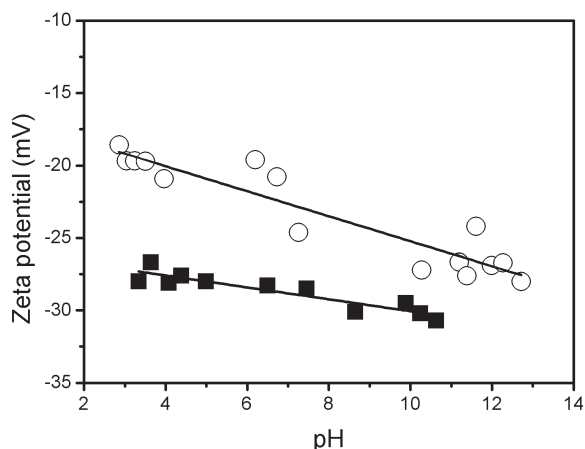
3 Zeta potential

4 The zeta potential (ζ) of organoclay Bent-0.8 was less
5 negative than the ζ of the starting clay throughout the pH
6 range studied (Figure 8). In order to produce a variation
7 in this potential, the adsorption of an ion with a charge
8 opposite to that of the layer (in this case, a cation) must
9 occur at a distance smaller than the thickness of the
10 Stern layer (Jouniaux and Ishido, 2012). Inorganic
11 cations are hydrophilic, adsorbed with their hydration
12 spheres forming outer sphere complexes outside of the
13 Stern layer. Moreover, surfactant molecules are hydro-
14 phobic and are adsorbed in a specific way, forming inner
15 sphere complexes with the negative charges of the
16 layers, which produce an increase in the ζ .

17 Adsorption model

18 The processes that are possible as the SL value
19 increases were deduced by analysing the data shown in
20 Figure 9 and the scheme illustrated in Figure 10. Note
21 that Figure 9 is not an adsorption isotherm, as the
22 horizontal axis does not represent surfactant concentra-
23 tion at equilibrium. Figure 9 shows the variations of the
24 quantity of surfactant and bromide adsorbed by the
25 different mechanisms with respect to the amount of
26 surfactant added initially.

27 When the SL value was small (Figure 10b), surfactant
28 adsorption occurred with the release of Na^+ to super-
29 natant solution, as was verified by chemical analysis and
30 XPS results. The large adsorption energies determined
31 from the adjustment of adsorption isotherms and the
32 variations in bending energy indicate that the process
33 carried out in this stage was not simply an exchange of
34 cations. The zeta potential results suggest that it was a
35 specific adsorption, involving the formation of an inner
36 sphere complex and the transfer of charge between the
37



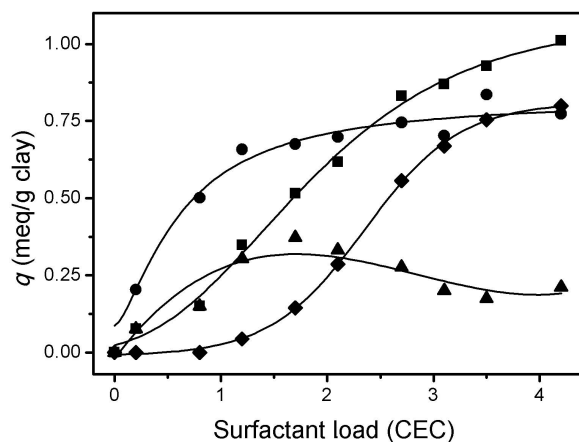
38 Figure 8. Zeta potential vs. pH. Comparison of the starting clay
39 (■) with the organoclay Bent-0.4 (○).

40 surfactant and the clay mineral. This process (strong
41 adsorption) continued until it reached a value of SL = 1.
42 Surfactant molecules adsorbed through this mechanism
43 are referred to as 'HDTMA⁺(CE).'

44 Another adsorption mechanism may be proposed
45 based on TG results, the adjustment of data given by
46 the Dubinin-Raduskevich adsorption model, and the
47 binding energy bands corresponding to nitrogen atoms in
48 XPS studies, in which the surfactant in the solution
49 interacts, through Van der Waals forces, with alkyl tails
50 of previously adsorbed surfactant cations. This process
51 (weak adsorption) was observed throughout the SL range
52 studied. Surfactant molecules adsorbed through this
53 mechanism were referred to as 'HDTMA^{total}(VdW).'

54 From the total amount of surfactant molecules
55 adsorbed through Van der Waals forces, a fraction was
56 present as cations, and another fraction formed ion pairs
57 with bromide anions. For an SL value < the CEC
58 (Figure 10a), the organoclay carried a net negative
59 charge, keeping Br^- anions from getting close to it.
60 Weak adsorption of ionic pairs, quantified by the
61 decrease of bromide in supernatant solutions and
62 corroborated by the presence of the peak corresponding
63 to bromine in XPS spectra, started when SL > 1 and
64 increased with SL in the studied range (Figure 10d).
65 Surfactant molecules adsorbed through this mechanism
66 were referred to as 'HDTMA⁺Br⁻(VdW).'

67 The interaction mechanisms between the surfactant
68 and the clay are summarized in Table 2. The difference
69 between HDTMA^{total}(VdW) and HDTMA⁺Br⁻(VdW)
70 was the amount of surfactant adsorbed by VdW forces
71 that did not form ion pairs. This type of adsorption was
72 observed throughout the SL range studied, with a
73 maximum at an intermediate value (SL \approx 1.7 CEC)
74 (Figure 9). Surfactant molecules adsorbed through this
75 mechanism were referred to as 'HDTMA⁺(VdW).'



76 Figure 9. Different forms of surfactant adsorption:
77 HDTMA⁺(CE) (●), HDTMA^{Total}(VdW) (■),
78 HDTMA⁺Br⁻(VdW) (▲), and HDTMA⁺(VdW) (◆): amounts
79 adsorbed per mass of clay in relation to the amount of surfactant
80 added initially.

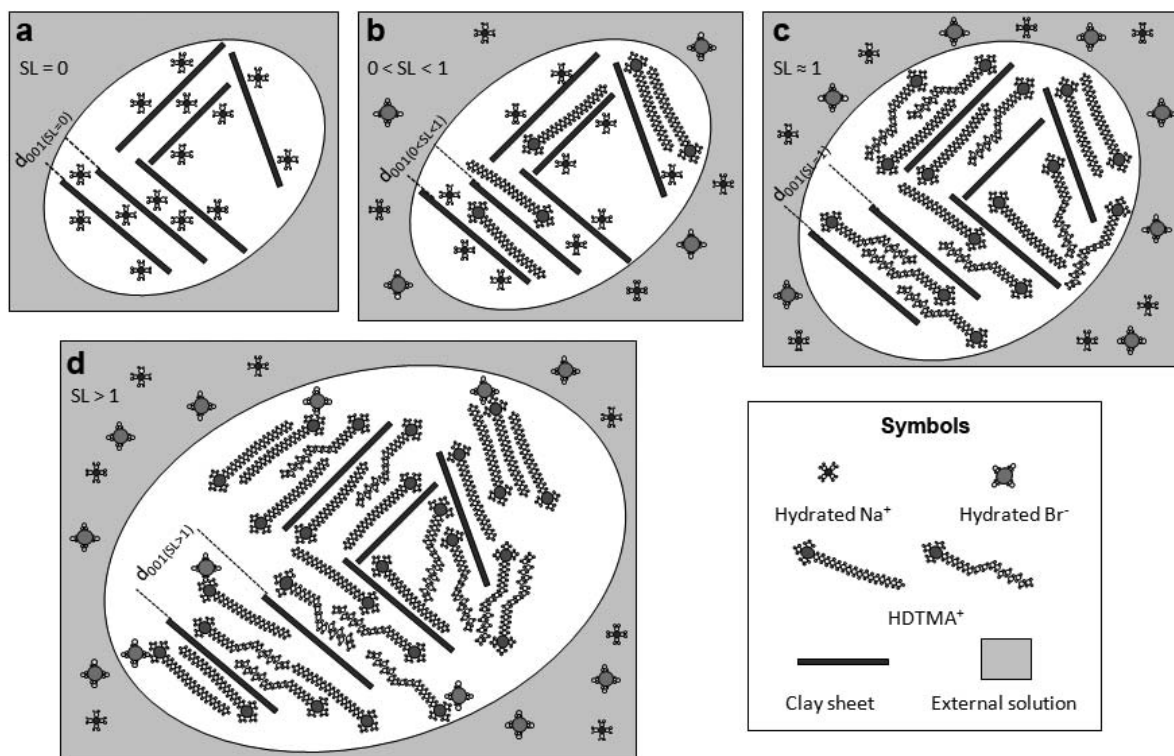


Figure 10. Schematic representation of the process of adsorption of surfactant on the surface of montmorillonite.

CONCLUSIONS

Organoclays containing different amounts of organic compounds were synthesized using $\text{HDTMA}^+\text{Br}^-$ as the surfactant. Two different mechanisms of surfactant adsorption were observed and the fractions adsorbed by each mechanism were quantified, using different characterization techniques.

Maximum adsorbed amounts and the adsorption energies involved in each mechanism were determined applying Langmuir and Dubinin-Raduskevich adsorption models to the data.

The present study verified that surfactant adsorption in the interlayer space of the clay mineral is produced by a 'strong' adsorption mechanism, in which the surfactant forms an inner sphere and/or charge-transfer complex with clay layers, as corroborated by ζ potential and XPS measurements. The study also confirmed the existence of a 'weak' adsorption mechanism, by Van der Waals-type interactions between carbon tails of the surfactant molecules in solution and the molecules previously adsorbed by the 'strong' mechanism.

Based on these results, the proposed interaction mechanism between the organic surfactant and the clay mineral is characterized qualitatively and, for the first time, quantitatively.

REFERENCES

- Akçay, G., Akçay, M., and Yurdakoç, K. (2006) The characterization of prepared organomontmorillonite (DEDMAM) and sorption of phenoxyalkanoic acid herbicides from aqueous solution. *Journal of Colloid and Interface Science*, **296**, 428–433.
- Azejjel, H., del Hoyo, C., Draoui, K., Rodríguez-Cruz, M.S., and Sánchez-Martín, M.J. (2009) Natural and modified clays from Morocco as sorbents of ionizable herbicides in aqueous medium. *Desalination*, **249**, 1151–1158.
- Bilgiç, C. (2005) Investigation of the factors affecting organic cation adsorption on some silicate minerals. *Journal of Colloid and Interface Science*, **281**, 33–38.
- Briggs, D. (1998) *Surface Analysis of Polymers by XPS and Static SIMS*. Cambridge University Press, New York.
- Carrado, K.A. (2000) Synthetic organo- and polymer-clays: preparation, characterization, and materials applications. *Applied Clay Science*, **17**, 1–23.
- de Paiva, L.B., Morales, A.R., and Valenzuela Díaz, F.R. (2008) Organoclays: Properties, preparation and application. *Applied Clay Science*, **42**, 8–24.
- Donat, R., Akdogan, A., Erdem, E., and Cetisli, H. (2005) Thermodynamics of Pb^{2+} and Ni^{2+} adsorption onto natural bentonite from aqueous solutions. *Journal of Colloid and Interface Science*, **286**, 43–52.
- Giles, C., Smith, D., and Huitson, A. (1974) A general treatment and classification of the solute adsorption isotherm. I. Theoretical. *Journal of Colloid and Interface Science*, **47**, 755–765.
- He, H., Ding, Z., Zhu, J., Yuan, P., Xi, Y., Yang, D., and Frost, R.L. (2005) Thermal characterization of surfactant-modified montmorillonites. *Clays and Clay Minerals*, **53**, 287–293.

- 1 He, H., Frost, R.L., Bostrom, T., Yuan, P., Duong, L., Yang D.,
2 Xi, Y., and Klopogge, J.T. (2006) Changes in the
3 morphology of organoclays with HDTMA⁺ surfactant
4 loading. *Applied Clay Science*, **31**, 262–271.
- 5 He, H., Zhou, Q., Frost, R.L., Wood, B.J., Duong, L.V., and
6 Klopogge, J. T. (2007) A X-ray photoelectron spectroscopy
7 study of HDTMAB distribution within organoclays.
8 *Spectrochimica Acta Part A: Molecular and Biomolecular
9 Spectroscopy*, **66**, 1180–1188.
- 10 Jouniaux, L. and Ishido, T. (2010) Electrokinetics in earth
11 sciences: A tutorial. *International Journal of Geophysics*,
12 Volume 2012, 16 pages, doi: 10.1155/2012/286107.
- 13 Liu, G., Wu, S., van de Ven, M., Molenaar, A., and Besamusca,
14 J. (2010) Characterization of surfactant on montmorillonite
15 nanoclay to be used in bitumen. *Journal of Materials in
16 Civil Engineering*, **22**, 794–799.
- 17 Mahramanlioglu, M., Kizilcikli, I., and Bicer, I. (2002)
18 Adsorption of fluoride from aqueous solution by acid
19 treated spent bleaching earth. *Journal of Fluorine
20 Chemistry*, **115**, 41–47.
- 21 Seki, Y. and Yurdakoç, K. (2005) Paraquat adsorption onto
22 clays and organoclays from aqueous solution. *Journal of
23 Colloid and Interface Science*, **287**, 1–5.
- 24 Su, K., Radian, A., Mishael, Y., Yang, L., and Stucki, J.W.
25 (2012) Nitrate reduction by redox-activated, polydiallyldi-
26 methylammonium-exchanged ferruginous smectite. *Clays
27 and Clay Minerals*, **59**, 464–472.
- 28 Tahani, A., Karroua, M., Van Damme, H., Levitz, P., and
29 Bergaya, F. (1999) Adsorption of a cationic surfactant on
30 Na-montmorillonite: Inspection of adsorption layer by X-ray
31 fluorescence spectroscopies. *Journal of Colloid and
32 Interface Science*, **216**, 242–249.
- 33 Xi, Y., Martens, W., He, H., and Frost, R.L. (2005)
34 Thermogravimetric analysis of organoclays intercalated
35 with the surfactant octadecyltrimethylammonium bromide.
36 *Journal of Thermal Analysis and Calorimetry*, **81**, 91–97.
- 37 Yariv, S., Lapidés, Y., and Borisover, M. (2012) Thermal
38 analysis of tetraethylammonium and benzyltrimethylammo-
39 nium montmorillonites. *Journal of Thermal Analysis and
40 Calorimetry*, **110**, 385–394.
- 41 (Received 4 July 2012; revised 24 January 2013; Ms. 687;
42 AE: H. He)
- 43
44
45
46
47
48
49
50
51
52
53
54
55
56
57